

# Experimental Studies on the Enhancement of Permeability of Anthracite by Acidizing: A Case Study in the Daning Block, Southern Qinshui Basin

Zhiqi Guo, Yunxing Cao, Shi Dong, and Zheng Zhang\*



Cite This: *ACS Omega* 2021, 6, 31112–31121



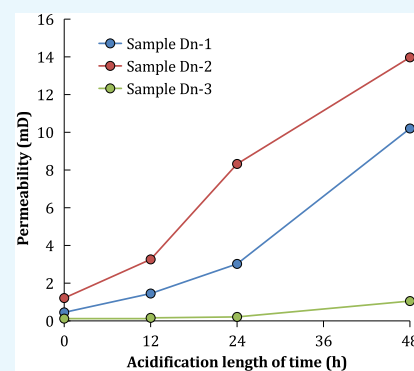
Read Online

ACCESS |

Metrics & More

Article Recommendations

**ABSTRACT:** As the most active and top producing area of coalbed methane (CBM) in China, the southern Qinshui Basin (SQB) is dominated by anthracite. Due to the low permeability of coals, plenty of non-gas-producing and low production CBM wells exist in the SQB. The permeability enhancement through some technological means is the key to increasing the CBM production of this area. In this paper, some typical anthracites were selected from the Daning block of the SQB to assess the effect of acidification treatments on permeability enhancement. The maceral composition determination shows that approximately 15% of minerals exist in the collected coal samples, and the X-ray diffractometer (XRD) results reveal that the minerals consist primarily of clay minerals, along with a little amount of quartz, calcite, and dolomite. Two types of acidizing fluids were used to conduct acidification treatments on the anthracites for different lengths of time. The  $N_2$  permeability of the anthracites before and after acidification was measured and compared. The results show that the original samples exhibit low permeability. As the acidification time increases, the permeability of all of the samples shows an increasing trend, and the acid sensitivity index  $I_a$  increases rapidly first and then levels off, and finally approaches 1. After 48 h of acidification, the samples show an increase ranging from 8.75 to 22.67 times (avg. 14.3 times) the original permeability. The permeability enhancement of the SQB anthracites is mainly attributed to the dissolution of acid-soluble minerals in the cleat system of coal. The minerals in the cleats are completely or partially dissolved by the acids, generating some soluble and insoluble substances; when the fluid flows through, the cleat space is reallocated. Overall, the cleat demineralization by acids frees up a lot of cleat spaces, leading to an increase in cleat connectivity. As a result, the fluid movement becomes smooth and the permeability of coal improves.



## INTRODUCTION

The commercial extraction of methane from coal beds is now well established in a number of countries throughout the world.<sup>1–4</sup> The global coalbed methane (CBM) resources estimated by the International Energy Agency (IEA) amount to 263.8 trillion  $m^3$ . The United States, Canada, Australia, China, and European countries such as Germany and the United Kingdom have all achieved the commercial development of CBM.<sup>5,6</sup> Due to mine-safety considerations, as well as energy demand and environmental benefits, the CBM development has been attached great importance by the Chinese government in the past decade. According to the fourth resource evaluation results conducted by the Ministry of Land and Resources of China, the CBM resources of China are 30.05 trillion  $m^3$ , and the recoverable resources are 12.5 trillion  $m^3$ , ranking third in the world.<sup>7</sup> Since 2008, the CBM production from surface wells of China has risen from 0.5 to 5.46 billion  $m^3$  in 2019.<sup>8</sup>

The Qinshui Basin possesses approximately 3.28 trillion  $m^3$  CBM resources.<sup>9</sup> As the largest and the most mature CBM development basin in China at present, the Qinshui Basin

accounts for 80% of CBM production of China.<sup>10</sup> The most successful CBM commercial development regions in the Qinshui Basin are in the southern portion, i.e., the southern Qinshui Basin (SQB).<sup>11</sup> The maximum vitrinite reflectance ( $R_{o,max}$ ) of coals in the SQB is between 2.0 and 4.0%,<sup>12</sup> and mostly exceeds 3.0%, reaching the anthracite stage. Though more than 8000 surface CBM-producing wells have been drilled in the SQB, the total production is still unsatisfactory because the number of non-gas-producing and low production wells accounts for up to 50–75% of the total.<sup>13</sup> Previous studies have shown that the key determinant for the gas production rate from a gas-bearing coal deposit is coal permeability.<sup>1,14</sup> Therefore, the overall low permeability of

**Received:** August 20, 2021

**Accepted:** November 3, 2021

**Published:** November 11, 2021



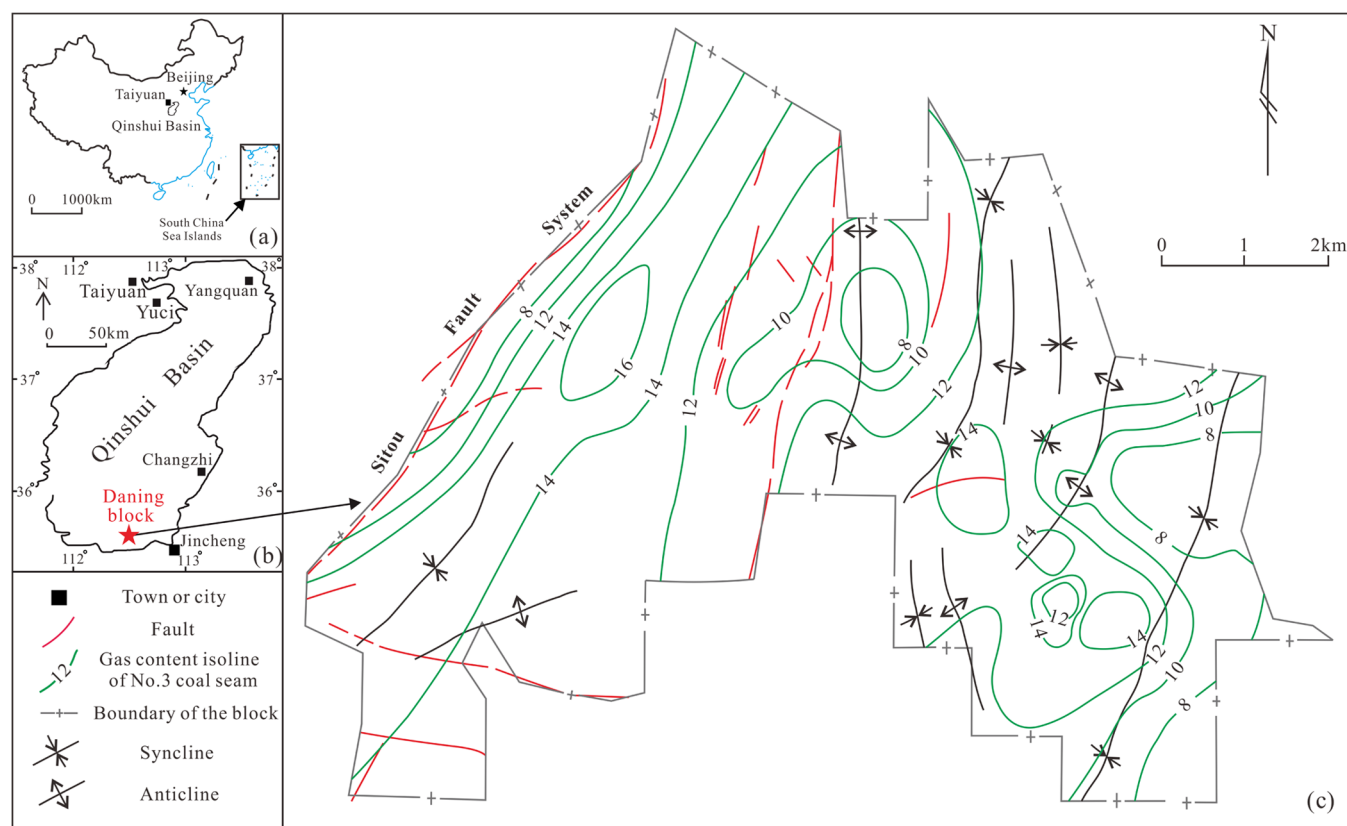


**Figure 1.** (a) Location of the Qinshui Basin in China, (b) outline of the Qinshui Basin and the location of the Daning block, and (c) structure outline of the Daning block and the gas content isoline of no. 3 coal seam.

high-rank coal is considered to be the vital reason for the low CBM production in the SQB.<sup>15–17</sup>

Due to low permeability, more than 96% CBM wells in China rely on fracturing stimulation technology to improve the permeability of coal seam.<sup>18</sup> The routine fracturing technology applied to coal seam is hydraulic fracturing, which uses surface high-pressure pumps to force fracturing fluid containing sand particles into the coal seam at high pressure to cause the coal seam to crack and produce conductive fractures.<sup>19</sup> The sand particles acting as a “proppant” are left in the coal seam as the fracturing fluid flows back to keep the newly formed fractures open and conductive. In general, about 98.5% of the hydraulic fracturing fluid is water and sand, and additives make up the rest 1.5%. The additives commonly consist of a variety of chemicals mainly aimed at structuring the fluid and assisting the delivery of the sand.<sup>20</sup>

The natural cleat system in the coal, including face cleat and butt cleat, plays a major role in determining permeability.<sup>1,14,21,22</sup> Previous studies have discovered that the cleat system in the coal is usually mineralized to varying degrees by various minerals, which occlude cleat porosity and reduce the permeability of the coal. Highly mineralized cleats can lead to low permeability of coals.<sup>21,23–25</sup> Hence, cleat demineralization by acids provides a possibility for improving coal permeability through increasing cleat connectivity and/or creating additional flow channels.<sup>19</sup> Utilization of acidification treatments to enhance permeability has been applied to conventional sandstone<sup>26–28</sup> and carbonate reservoirs.<sup>29–33</sup> In recent years, this technology has been attempted to be applied to enhancing coal permeability.<sup>19,22,34–36</sup>

Many previous studies have verified that the natural fractures in the coals of the SQB are filled with various minerals, such as carbonate (e.g., calcite, dolomite), oxide (e.g., hematite, quartz), sulfide (e.g., pyrite), and silicate minerals (e.g., kaolinite, illite).<sup>17,37,38</sup> The presence of these highly mineralized fractures significantly reduces the permeability of coals of the SQB. In this paper, some typical anthracites of the Daning block in the SQB were selected to assess the effect of acidification treatments on permeability enhancement. In addition, the mechanism of permeability enhancement of the SQB anthracite by acidizing was tentatively explored. The results can help improve the formulation of fracturing fluid applied to high-rank coals of the SQB.

## ■ GEOLOGICAL SETTINGS

The Daning block, covering an area of approximately 38.82 km<sup>2</sup>, is located in the southern Qinshui Basin (Figure 1b), which is a tectonic basin formed on the basement of the Late Paleozoic era.<sup>17</sup> The Daning block is situated at the junction of the southern end of Taihang Mountain and the northeastern edge of Zhongtiao Mountain.<sup>9</sup> The stratum of the Daning block slopes from south to north. The dip of the stratum is generally within 10° and can be over 20° locally due to structural influence. The eastern part of the block is dominated by folds with axial striking NE–SW or near N–S; the western part develops faults striking NE–SW, NNE–SSW, or W–E (Figure 1c). The Sitou fault system constitutes the western boundary of the block and affects the gas content of the coal seam in the block (Figure 1c).

The strata in the study area include Ordovician Fengfeng formation (O<sub>2f</sub>), Carboniferous Benxi formation (C<sub>2b</sub>),

Carboniferous-Permian Taiyuan formation ( $C_2$ - $P_{1t}$ ), Permian Shanxi ( $P_{1s}$ ), Xiashihezi ( $P_{1x}$ ), Shangshihexi ( $P_{2s}$ ), and Shiqianfeng ( $P_{2sh}$ ) formations, and Quaternary from bottom to top. The main coal-bearing strata are  $C_2$ - $P_{1t}$  and  $P_{1s}$  formations (Figure 2). The no. 3 coal seam in  $P_{1s}$  is the target layer for CBM exploitation in this block.

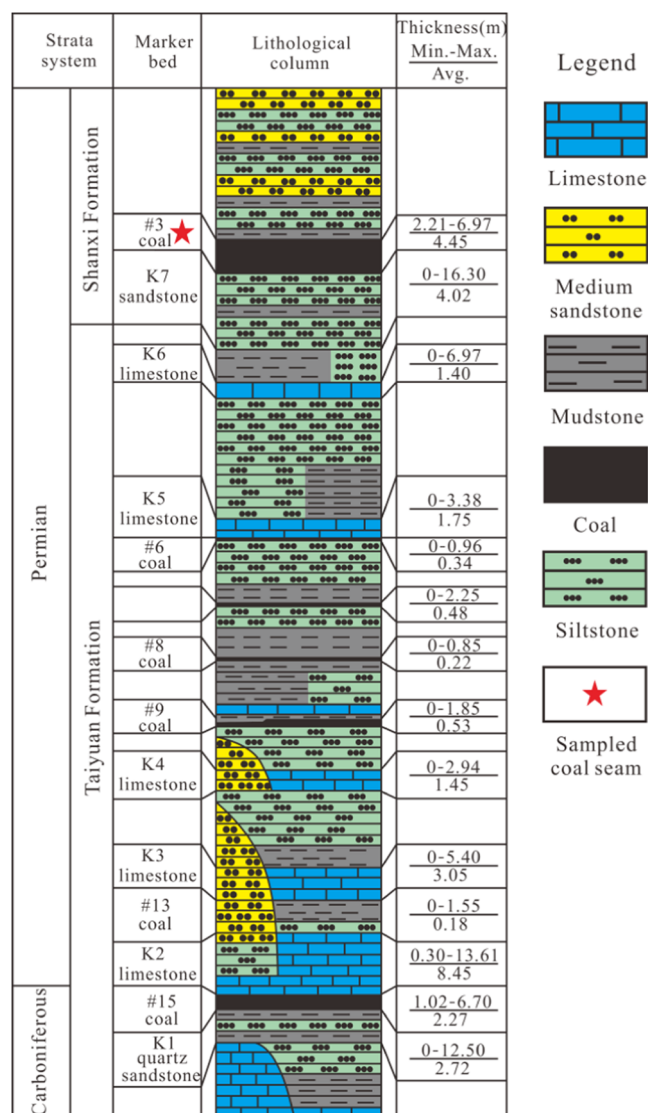


Figure 2. Stratigraphic column of coal-bearing strata in the Daning block and the sampled section.

The thickness of no. 3 coal seam in this block varies from 2.21 to 6.97 m, averaging 4.45 m. The burial depth is approximately between 100 and 600 m. The maximum vitrinite reflectance ( $R_{o,max}$ ) ranges from 2.95 to 3.36% (avg. 3.17%), indicating that the coal in this region is typical anthracite. The well testing permeability of no. 3 coal seam is from 0.10 to 6.49 mD with an average value of 0.96 mD. The reservoir pressure obtained from well testing varies from 0.67 to 3.19 (avg. 1.62) MPa, and the reservoir pressure gradient ranges from 0.15 to 0.82 (avg. 0.43) MPa/100 m. The gas content (dry ash-free basis,  $G_{daf}$ ) of no. 3 coal seam ranges from 5.56 to 17.57  $m^3/t$  with an average of 12.83  $m^3/t$ . The gas content inside the block is better than that near the boundary and is commonly low near the faults (Figure 1c).

## SAMPLES AND METHODS

**Sample Collection and Preparation.** In this study, a total of three fresh coal samples (DN-1, DN-2, and DN-3) were collected from the underground coal mine in the Daning block. All of the three samples were collected from the no. 3 coal seam in Shanxi Formation (Figure 2). The collected coal samples were big blocks with approximate dimensions of 250 mm  $\times$  250 mm  $\times$  200 mm. To prevent oxidation and preserve the natural moisture content during transport, the coal samples were wrapped with a white preservative film and then placed in black plastic bags immediately after being removed from the working faces. Samples were then sent to the laboratory for sample preparation.

For each big block of sampled coal, a horizontal core was carefully drilled with an approximate diameter of 2.5 cm and length of 4–5 cm, parallel to the bedding plane of the coal sample. Some small block samples with approximate dimensions of 2 cm  $\times$  2 cm  $\times$  2 cm were taken from alongside the cores, and these were crushed and sieved to different sizes for use in other experiments: <1 mm for maceral group composition quantifications and  $R_{o,max}$  measurements, 200 mesh for powder X-ray diffraction (XRD) and proximate analysis, and 10–20 mesh for static leaching experiments of coal fines.

**Proximate and Petrology Analysis.** Proximate analysis measurements of the coal samples including ash yield, moisture, and volatile matter were performed following the Chinese standard GB/T 212-2008.  $R_{o,max}$  measurements and maceral group composition determination were performed using a Leitz MPV-3 photometer microscope, according to the Chinese standards of GB/T 6948-2008 and GB/T 8899-2013, respectively.

Mineral compositions of the coal samples were determined using a D8 DISCOVER X-ray diffractometer made by Bruker, Germany. Prior to XRD analysis, low-temperature ashing of the powdered coal samples was carried out using a YAMATO PR301 plasma asher. The XRD analysis procedure and semiquantitative analysis are described in detail in Li et al.<sup>39</sup>

**Static Leaching Experiments of Coal Fines.** In the oil field, the mixed acid of hydrofluoric acid (HF) and hydrochloric acid (HCl) is often referred to as “mud acid”, which is used to remove mud blockage and increase the permeability of mud and sandstone formations, thus facilitating water injection or oil production. HCl in the mud acid can dissolve the carbonate minerals and iron and aluminum compounds in the formations, and HF can dissolve the clay and silicate minerals. Considering that the reaction speed of HCl and HF is too fast, and  $CH_3COOH$  can slow down the dissolution speed, so a certain amount of  $CH_3COOH$  was added to the acid solution formula in this study. KCl acting as a stabilizer is a common additive in the fracturing fluid.

The static leaching experiments of coal fines were used to investigate the coal dissolution effect in different types of mixed acids. An appropriate amount of fresh block coal from the Daning block was chosen, crushed, and sieved into particles with sizes between 10–20 mesh. Then, the crushed coal particles were dried in a drying oven at 60 °C for 12 h. The dried coal particles were divided into 36 subsamples, and each subsample weighs 5 g, accurate to 0.001 g. Next, each subsample was soaked in 50 mL of different mixed acids (Table 1) for different lengths of time (Table 2) at ambient pressure (1 atm) and constant temperature of 30 °C, which

**Table 1. Formula of the Mixed Acid**

acid	type of mixed acid					
	A (%)	B (%)	C (%)	D (%)	E (%)	F (%)
HF	3	5	6	3	6	2
HCl	3	2	3	6	0	5
CH <sub>3</sub> COOH	3	2	0	0	3	2

**Table 2. Dissolution Rate of Daning Coal Fines in Different Mixed Acids**

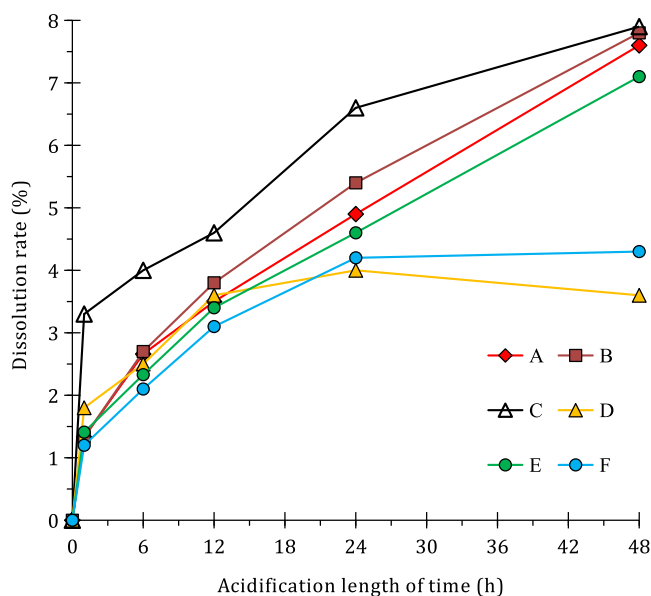
time (h)	type of mixed acid					
	A	B	C	D	E	F
1	1.33	1.33	3.30	1.80	1.41	1.20
6	2.66	2.70	4.00	2.50	2.33	2.10
12	3.50	3.80	4.60	3.60	3.40	3.10
24	4.90	5.40	6.60	4.00	4.60	4.20
48	7.60	7.80	7.90	3.60	7.10	4.30

was provided by a thermostatic water bath. Then, the crushed coal particles and the leachate were separated using quantitative filter paper with a pore size of 30–50  $\mu\text{m}$ . The coal fines along with the filter paper were dried at 80  $^{\circ}\text{C}$  until the mass is constant and weighed to determine the mass variation before and after acidizing. The dissolution rate ( $R_d$ ) was calculated according to eq 1, as follows

$$R_d = \frac{w_1 - (w_2 - w_0)}{w_1} \times 100\% \quad (1)$$

where  $R_d$  is the dissolution rate of the coal, %;  $w_1$  is the weight of the coal before acidizing, g;  $w_2$  is the weight of the coal after acidizing, g; and  $w_0$  is the weight of the filter paper, g.

The calculated dissolution rate of Daning coal in different types of mixed acids is presented in Table 2 and Figure 3. After acidizing for 48 h, the dissolution rate of Daning coal in mixed acids A, B, and C is the highest with values of 7.60, 7.80, and 7.90%, respectively. From the dissolution rate curves in Figure 3, it can be seen that the slopes of curves of mixed acids A and

**Figure 3.** Dissolution rate of Daning coal fines in different mixed acids.

B are stable, reflecting that the reactions between the coal fines and acids are steady. Therefore, the mixed acids of type A and type B were finally selected to conduct “core acidizing experiments” in the permeability measurements.

**Permeability Measurements.** The  $\text{N}_2$  permeability of each coal sample was measured using the routine core analysis methods by the Chinese Oil and Gas Industry Standard (SY/T) 5336-1996. The apparatus used for the  $\text{N}_2$  permeability experiment mainly consists of a  $\text{N}_2$  supply cylinder, a core holding unit, a confining pressure oil pump, a pressure transducer, a gas flow meter, and a computerized system for data acquisition and process control (Figure 4). Prior to  $\text{N}_2$  permeability measurement, the apparatus was checked carefully to make sure it was well sealed.

In this study, two sets of  $\text{N}_2$  permeability experiments were performed on the coal cores. One was carried out under the condition that the coal sample cores were not acidified, and the other under the condition that the coal sample cores were acidified for different lengths of time. The whole experiment was divided into four steps. First of all, the coal sample cores were dried for 24 h at 60  $^{\circ}\text{C}$  in a drying oven and then evacuated for 16 h. Second, the coal sample core was placed into the core holding unit for  $\text{N}_2$  permeability measurement under an inlet pressure of 0.5 MPa, an outlet pressure of 0.1 MPa, and a constant confining pressure of 4.0 MPa; the  $\text{N}_2$  permeability measurement process was terminated when the gas flow rate was stable. Third, the coal sample core was taken out from the core holding unit and soaked in the acidizing fluid, and the soaking length of time was set to 12, 24, and 48 h. Finally, after each soaking, the first and the second steps were repeated in sequence. The acidizing fluid used for soaking samples DN-1 and DN-2 was “3%HF + 3%HCl + 3%CH<sub>3</sub>COOH + 2%KCl” (A type acidizing fluid) and the acidizing fluid of “5%HF + 2%HCl + 2%CH<sub>3</sub>COOH + 2%KCl” (B type acidizing fluid) was used for soaking sample DN-3.

During the process of  $\text{N}_2$  permeability measurement, data such as the gas flow rate, inlet pressure, and outlet pressure were automatically recorded by the computerized system. The  $\text{N}_2$  permeability of the coal sample core can be calculated by the following formula

$$K = \frac{2p_0 q \mu L \times 10^2}{A(p_1^2 - p_0^2)} \quad (2)$$

where  $K$  is the  $\text{N}_2$  permeability of the coal sample, mD ( $10^{-3} \mu\text{m}^2$ );  $p_0$  and  $p_1$  are gas pressures at the outlet and the inlet, MPa, respectively;  $A$  and  $L$  are the cross-sectional area,  $\text{cm}^2$ , and the length, cm, of the coal sample, respectively;  $\mu$  is the viscosity of  $\text{N}_2$  under measured temperature, mPa·s; and  $q$  is the flux of  $\text{N}_2$ ,  $\text{cm}^3/\text{s}$ .

## RESULTS AND DISCUSSIONS

**Coal Properties and Mineral Compositions.** The measurement results of proximate analysis, maceral group compositions, and  $R_{o,\text{max}}$  are presented in Table 3. Proximate analysis shows that moisture contents of the coal samples are between 0.92 and 2.11%, ash yields 10.11–15.16%, volatile matter yields 9.42–16.20%, and fixed carbon contents 83.80–90.58%, respectively. The maceral compositions data show that vitrinite contents account for 61.2–68.1%, inertinite contents between 16.8 and 17.6%, and mineral contents 14.9–16.2%,

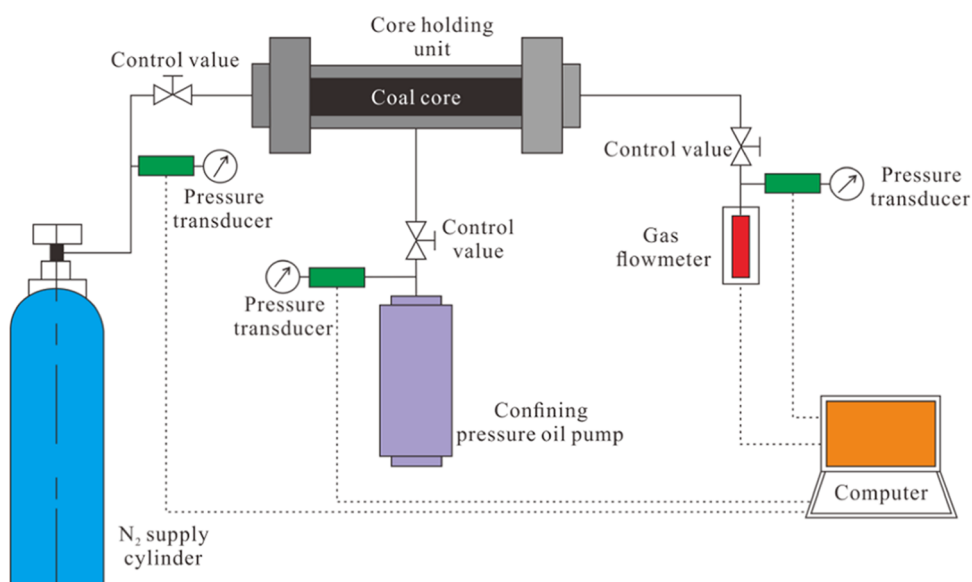


Figure 4. Schematic diagram of the  $N_2$  permeability experiment of the coal core.

Table 3. Coal Composition,  $R_{o,max}$ , and Proximate Analysis of the Coal Samples from the Daning Block<sup>a</sup>

coal samples	maceral and mineral (vol %)				$R_{o,max}$ (%)	proximate analysis (wt %)			
	V	I	L	M		$M_{ad}$	$A_d$	$V_{daf}$	$FC_{daf}$
Dn-1	61.2	17.6	0	16.2	3.05	0.92	10.11	16.20	83.80
Dn-2	67.5	16.8	0	15.7	2.95	2.11	15.16	13.09	86.91
Dn-3	68.1	16.8	0	14.9	3.00	1.65	12.92	9.42	90.58

<sup>a</sup> $R_{o,max}$  = the max vitrinite reflectance; V = vitrinite; I = inertinite; L = liptinite; M = mineral;  $M_{ad}$  = moisture (air-dried basis);  $A_d$  = ash (dry basis);  $V_{daf}$  = volatile matter (dry, ash-free basis); and  $FC_{daf}$  = Fixed carbon (dry, ash free basis).

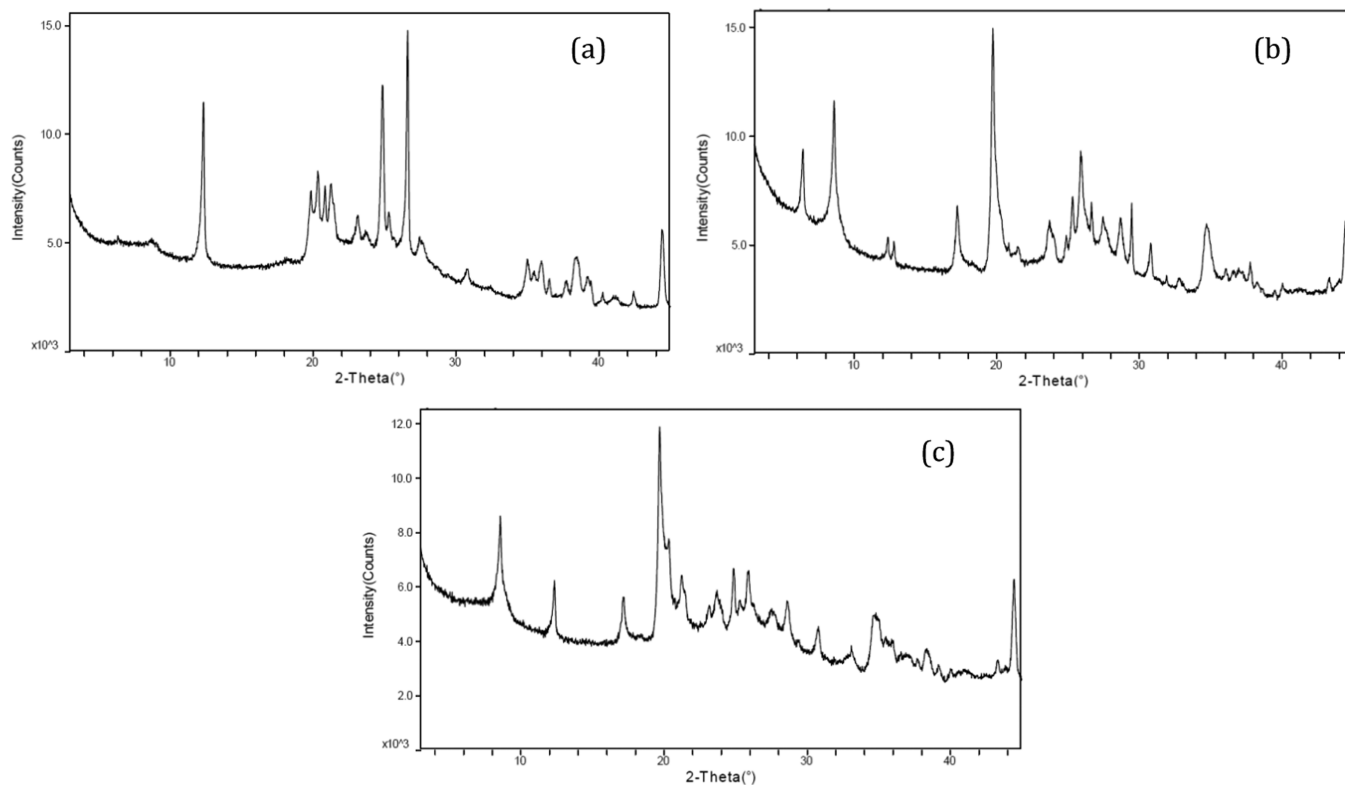


Figure 5. XRD spectra of coal samples from the Daning block. (a) Dn-1, (b) Dn-2, and (c) Dn-3.

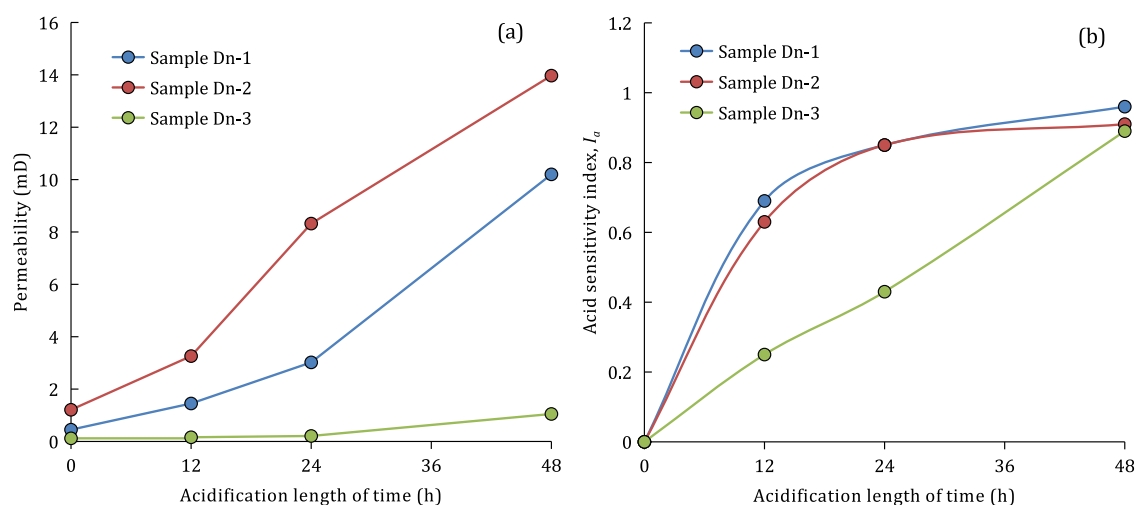
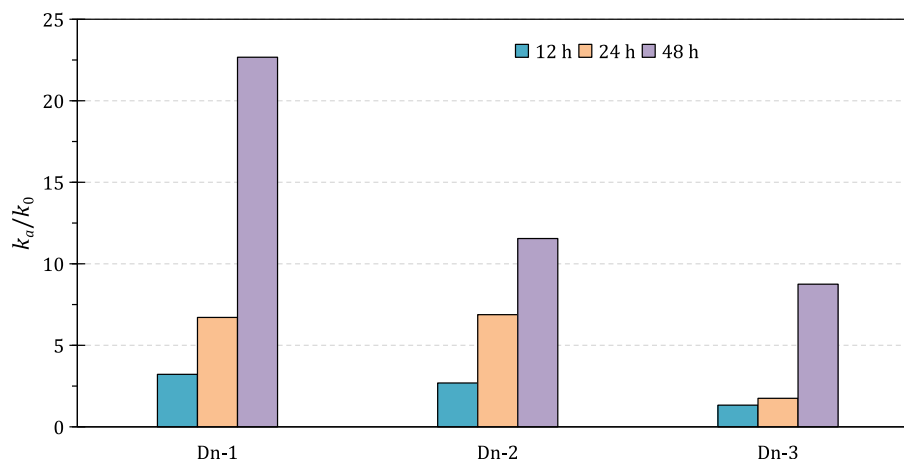
**Table 4. Mineralogical Proportions of the Coal Samples Determined by XRD from the Daning block (Unit in %)**

coal samples	quartz	calcite	dolomite	clay minerals			
				kaolinite	chlorite	illite	interstratified minerals
Dn-1	4	2	1	22	9	2	60
Dn-2	1	3	1	1	0	65	29
Dn-3	2	1	1	5	4	29	58

**Table 5. Measurement Results of N<sub>2</sub> Permeability of the Coal Samples before and after Acidification<sup>a</sup>**

coal samples	$k_0$	acid type	12 h			24 h			48 h		
			$k_a$	$R_e$	$I_a$	$k_a$	$R_e$	$I_a$	$k_a$	$R_e$	$I_a$
Dn-1	0.45	A	1.45	3.22	0.69	3.02	6.71	0.85	10.2	22.67	0.96
Dn-2	1.21	A	3.26	2.69	0.63	8.32	6.88	0.85	13.97	11.55	0.91
Dn-3	0.12	B	0.16	1.33	0.25	0.21	1.75	0.43	1.05	8.75	0.89

<sup>a</sup> $k_0$ , N<sub>2</sub> permeability of coal sample before acidification, mD;  $k_a$ , N<sub>2</sub> permeability of coal sample after different acidification length of time, mD;  $R_e = k_a/k_0$ ; and  $I_a$ , acid sensitivity index.

**Figure 6. Plots of the permeability (a) and acid sensitivity index (b) of coal samples versus acidification length of time.****Figure 7. Ratio change of  $k_a/k_0$  of coal samples with acidification length of time.**

respectively.  $R_{o,max}$  of the coal samples ranges from 2.95 to 3.05%, indicating that the coal samples are anthracites.

The XRD spectra of the coal samples are shown in Figure 5, and the interpreted mineral proportions are presented in Table 4. The results show that the mineral matters in the coals of the Daning block consist primarily of clay minerals, along with a little amount of quartz, calcite, and dolomite. For coal samples

of Dn-1 and Dn-3, the clay minerals are composed of interstratified clay minerals, along with varying amounts of kaolinite, chlorite, and illite. However, the clay minerals in the coal sample of Dn-2 mainly consist of vast illite and relatively lower interstratified minerals.

**Changes of Permeability after Acidizing.** The N<sub>2</sub> permeability of coal samples before and after acidizing is

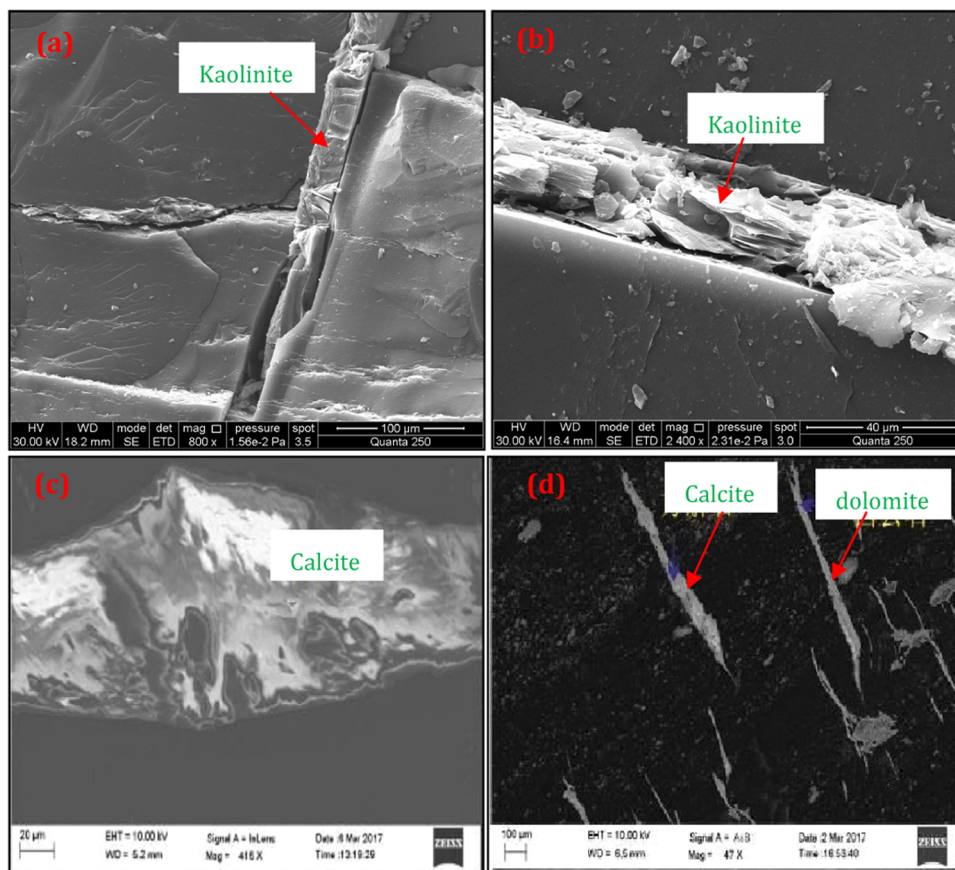


**Figure 8.** Scanning electron microscopy (SEM) images showing mineralized fractures (original from refs 17 and 38). (a) Kaolinite in the fracture, (b) kaolinite in the fracture, (c) calcite in the fracture, and (d) calcite and dolomite in the fractures. Panels (a, b) are reprinted from ref 17, Copyright (2018), with permission from Elsevier. Panels (c, d) are reprinted from ref 38, Copyright (2020), with permission from Elsevier.

presented in Table 5. The permeability of coal samples ( $k_0$ ) before acidification shows a low level with values ranging from 0.12 to 1.21 mD, averaging only 0.59 mD.  $k_0$  of the three coal samples takes on  $Dn-2 > Dn-1 > Dn-3$ . After acidizing the coal samples for different lengths of time, the permeability of coal samples ( $k_a$ ) was increased to varying degrees. It can be seen that the permeability of all of the samples shows an increasing trend as the acidification time increases. That is, the longer the acidification time, the greater the increase in permeability. Within the same acidification time, the permeability value is always maintained at  $Dn-2 > Dn-1 > Dn-3$  (Table 5 and Figure 6a). After 48 h of acidification, sample Dn-1 presents the largest increase in permeability, which increases from 0.45 to 10.2 mD, an increase of 21.67 times the original permeability; samples Dn-2 and Dn-3 have an increase of nearly 10 times (Figure 7). Obviously, acidification can significantly improve the permeability of anthracites of the SQB. In terms of acid type, type A acid is better than type B acid in improving the permeability of the coal samples (Table 5).

To characterize the sensitivity of coal reservoir permeability to acid treatments, a parameter named the acid sensitivity index ( $I_a$ ) is defined in this study, and the calculation formula is as follows

$$I_a = (k_a - k_0) / k_a$$

where  $k_a$  is the  $N_2$  permeability of the coal sample after acidification, mD;  $k_0$  is the  $N_2$  permeability of the coal sample

before acidification, mD; and  $I_a$  is the acid sensitivity index of the coal sample.

It can be seen that the acid sensitivity index  $I_a$  increases with the increase in acidification time (Figure 6b). The  $I_a$  of samples Dn-1 and Dn-2 is always maintained at the same level, and  $I_a$  of sample Dn-3 is significantly lower than the other two samples at most of the acidification times. It reflects that the permeability of sample Dn-3 is relatively insensitive to acid treatment. Overall, with the increase in acidification time,  $I_a$  increases rapidly first and then levels off, and finally approaches 1.

**Mechanism of Permeability Enhancement by Acidizing.** A coal reservoir is a dual-porosity system containing porous matrix blocks and a naturally fractured network known as cleats.<sup>40–43</sup> The complex natural cleats are widespread in coal reservoirs and play a crucial role in the permeability of coal reservoirs. However, lots of cleats in coal reservoirs are filled with various minerals such as carbonate (e.g., calcite, dolomite), oxide (e.g., hematite, quartz), sulfide (e.g., pyrite), and silicate minerals (e.g., kaolinite, illite).<sup>24,25</sup> The presence of these highly mineralized cleats may occlude fracture porosity and then reduce the permeability of coal reservoirs.<sup>19</sup>

As shown in Tables 3 and 4, the anthracites in this study contain approximately 15% minerals, which are primarily composed of clay minerals, along with a little amount of quartz, calcite, and dolomite. The previous studies in the SQB have verified that these minerals widely exist in the cleats and pores of anthracite (Figure 8).<sup>17,37,38</sup>

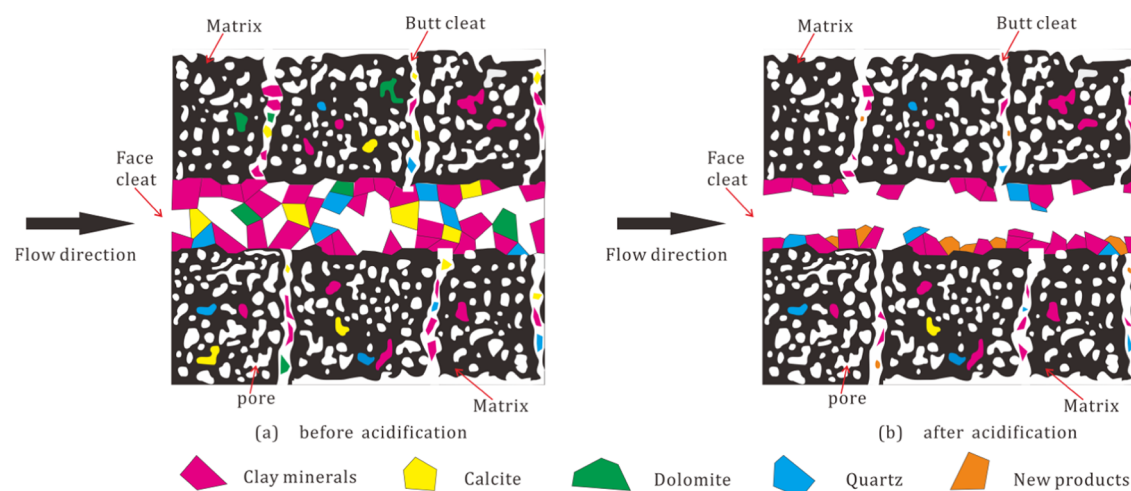
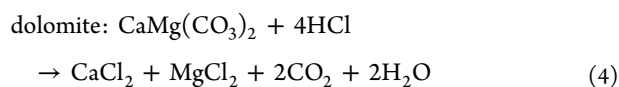
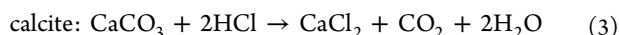


**Figure 9.** Graphical representation showing the solution of minerals in cleats and pores due to acidification. Distribution of minerals (a) before acidification and (b) after acidification.

During the acidification process, a large amount of acids (HCl, HF) enters the pores and cleats of the coal reservoirs and then reacts with the minerals. The possible chemical reaction equations involved are presented in eqs 3–7. Carbonate minerals are converted into water-soluble chlorides under the action of HCl (eqs 3 and 4). Quartz is converted into fluorosilicic acid under the slow dissolution of HF (eq 5). Kaolinite reacts with HF to generate fluorosilicic acid and insoluble aluminum fluoride (eq 6). Smectite reacts with HF to generate fluorosilicic acid and fluoroaluminate (eq 7).

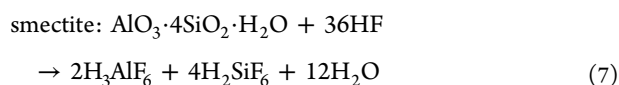
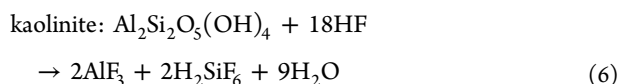
Acidification of carbonate minerals



Acidification of quartz



Acidification of clay minerals



The graphical representation showing the dissolution of acid-soluble minerals in cleats and pores is presented in Figure 9. As the channels of fluid flow, the cleats (face cleat and butt cleat) distributed between the coal matrix blocks were completely or partially filled with large amounts of minerals before acidification of coal samples. These minerals, including clay minerals, quartz, calcite, and dolomite, block the cleat space and seriously affect the movement of fluids. The anthracites in the study area have poor in situ cleat development and low permeability.<sup>17,44</sup> The presence of these highly mineralized cleats will undoubtedly lead to much lower permeability. With the action of acids, the minerals in the cleats are completely or partially dissolved. The carbonate minerals were completely dissolved and converted

into water-soluble chlorides, which were then carried away by the fluid flow. The quartz and clay minerals are partially dissolved, and it causes them to break up into small particles, among which some remain on the wall of the cleats and some become mobile and are carried away by the fluid flow. During the dissolution of clay minerals by acids, some insoluble substances such as aluminum fluoride ( $\text{AlF}_3$ ) were generated and accumulated on the surface of the lower wall of the cleat or carried away by the fluid flow. Overall, the cleat demineralization by acids frees up a lot of cleat spaces, leading to an increase in cleat connectivity. As a result, the fluid movement becomes smooth and the permeability of coal improves. During the acidification, some minerals in the pores of the matrix will also be dissolved by acids, which will improve the gas diffusion of coal.

## CONCLUSIONS

Mineral occlusions in cleats considerably reduce the permeability of anthracites in the SQB, influencing CBM production. In this work, some anthracites from the SQB were selected to assess the effect of acidification treatments on permeability enhancement. For all of the samples, an obvious increasing trend of permeability was obtained as the acidification time increased. The samples show an increase ranging from 8.75 to 22.67 times (avg. 14.3 times) the original permeability after 48 h of acidification. Overall, the acid sensitivity index  $I_a$  increases rapidly first and then levels off, and finally approaches 1. The permeability enhancement of the SQB anthracites is mainly attributed to the dissolution of acid-soluble minerals in the cleat system of coal. The minerals in the cleats are completely or partially dissolved by the acids, generating some soluble and insoluble substances; when the fluid flows through, the cleat space is reallocated. Overall, the cleat demineralization by acids frees up a lot of cleat spaces, leading to an increase in cleat connectivity. As a result, the fluid movement becomes smooth and the permeability of coal improves. Acidification treatments have an obvious effect on increasing the permeability of anthracites in the SQB.



## AUTHOR INFORMATION

### Corresponding Author

Zheng Zhang – Key Laboratory of Coalbed Methane Resources and Reservoir Formation Process, Ministry of Education of China, China University of Mining and Technology, Xuzhou 221116, China; [orcid.org/0000-0002-7146-0376](https://orcid.org/0000-0002-7146-0376); Email: [zccumt@cumt.edu.cn](mailto:zccumt@cumt.edu.cn)

### Authors

Zhiqi Guo – Key Laboratory of Coalbed Methane Resources and Reservoir Formation Process, Ministry of Education of China, China University of Mining and Technology, Xuzhou 221116, China

Yunxing Cao – School of Safety Science and Engineering, Henan Polytechnic University, Jiaozuo 454003, China

Shi Dong – Shanxi Lanhua Sci-tech Venture Co., Ltd., Jincheng 048000, China

Complete contact information is available at:

<https://pubs.acs.org/10.1021/acsomega.1c04539>

### Notes

The authors declare no competing financial interest.

## ACKNOWLEDGMENTS

This work was financially supported by the Science and Technology Key Special Project of Shanxi Province (No. 20111101003) and the Natural Science Foundation of China (No. 41802192).

## REFERENCES

- (1) Moore, T. A. Coalbed methane: a review. *Int. J. Coal Geol.* **2012**, *101*, 36–81.
- (2) Qin, Y.; Moore, T. A.; Shen, J.; Yang, Z.; Shen, Y.; Wang, G. Resources and geology of coalbed methane in China: a review. *Int. Geol. Rev.* **2018**, *60*, 777–812.
- (3) Tao, S.; Pan, Z. J.; Tang, S.; Chen, S. Current status and geological conditions for the applicability of CBM drilling technologies in China: a review. *Int. J. Coal Geol.* **2019**, *202*, 95–108.
- (4) Lupton, N.; Connell, L. D.; Heryanto, D.; Sander, R.; Camilleri, M.; Down, D. I.; Pan, Z. J. Enhancing biogenic methane generation in coalbed methane reservoirs – Core flooding experiments on coals at in-situ conditions. *Int. J. Coal Geol.* **2020**, *219*, No. 103377.
- (5) Hamawand, I.; Yusuf, T.; Hamawand, S. G. Coal seam gas and associated water: a review paper. *Renewable Sustainable Energy Rev.* **2013**, *22*, 550–560.
- (6) Gerami, A.; Mostaghimi, P.; Armstrong, R. T.; Zamani, A.; Warkiani, M. E. A microfluidic framework for studying relative permeability in coal. *Int. J. Coal Geol.* **2016**, *159*, 183–193.
- (7) Xu, F.; Xiao, Z.; Chen, D.; Yan, X.; Wu, N.; Li, X.; Miao, Y. Current status and development direction of coalbed methane exploration technology in China. *Coal Sci. Technol.* **2019**, *47*, 205–215.
- (8) Qin, Y. Strategic thinking on research of coal measure gas accumulation system and development geology. *J. China Coal Soc.* **2021**, 2387–2399.
- (9) Cai, Y.; Liu, D.; Yao, Y.; Li, J.; Qiu, Y. Geological controls on prediction of coalbed methane of No. 3 coal seam in Southern Qinshui Basin, North China. *Int. J. Coal Geol.* **2011**, *88*, 101–112.
- (10) Zhao, X.; Zhu, Q.; Sun, F.; Yang, Y.; Wang, B.; Zuo, Y.; Shen, J.; Mu, F.; Li, M. Practice and thought of coalbed methane exploration and development in Qinshui Basin. *J. China Coal Soc.* **2015**, *40*, 2131–2136.
- (11) Zhang, Z.; Qin, Y.; Bai, J.; Li, G.; Zhuang, X.; Wang, X. Hydrogeochemistry characteristics of produced waters from CBM wells in Southern Qinshui Basin and implications for CBM commingled development. *J. Nat. Gas Sci. Eng.* **2018**, *56*, 428–443.
- (12) Sun, F.; Wang, B.; Li, M.; Liang, H. Major geological factors controlling the enrichment and high yield of coalbed methane in the southern Qinshui Basin. *Acta Pet. Sin.* **2014**, *35*, 1070–1079.
- (13) Ye, J.; Lu, X. Development status and technical progress of China coalbed methane industry. *Coal Sci. Technol.* **2016**, *44*, 24–28.
- (14) Flores, R. M. *Coal and Coalbed Gas, Fueling the Future*; Elsevier Inc. Press: Boston, 2014.
- (15) Tao, S.; Tang, D.; Xu, H.; Gao, L.; Fang, Y. Factors controlling high-yield coalbed methane vertical wells in the Fanzhuang Block, Southern Qinshui Basin. *Int. J. Coal Geol.* **2014**, *134–135*, 38–45.
- (16) Zhao, X.; Yang, Y.; Sun, F.; Wang, B.; Zuo, Y.; Li, M.; Shen, J.; Mu, F. Enrichment mechanism and exploration and development technologies of high coal rank coalbed methane in south Qinshui Basin, Shanxi Province. *Pet. Explor. Dev.* **2016**, *43*, 332–339.
- (17) Zhang, Z.; Qin, Y.; Zhuang, X.; Li, G.; Wang, X. Poroperm characteristics of high-rank coals from Southern Qinshui Basin by mercury intrusion, SEM-EDS, nuclear magnetic resonance and relative permeability analysis. *J. Nat. Gas Sci. Eng.* **2018**, *51*, 116–128.
- (18) Zhang, S.; Liu, X.; Wen, Q.; Zhang, X.; Zhao, W.; Yuan, Y. Development situation and trend of stimulation and reforming technology of coalbed methane. *Acta Pet. Sin.* **2021**, *42*, 105–118.
- (19) Turner, L. G.; Steel, K. M. A study into the effect of cleat demineralisation by hydrochloric acid on the permeability of coal. *J. Nat. Gas Sci. Eng.* **2016**, *36*, 931–942.
- (20) King, G. E. *Hydraulic Fracturing Technology Conference*; Society of Petroleum Engineers: Woodlands, Texas, 2012.
- (21) Dawson, G. K. W.; Esterle, J. S. Controls on coal cleat spacing. *Int. J. Coal Geol.* **2010**, *82*, 213–218.
- (22) Balucan, R. D.; Turner, L. G.; Steel, K. M. Acid-induced mineral alteration and its influence on the permeability and compressibility of coal. *J. Nat. Gas Sci. Eng.* **2016**, *33*, 973–987.
- (23) Han, F.; Busch, A.; Krooss, B. M.; Liu, Z.; Van Wagoningen, N.; Yang, J. Experimental study on fluid transport processes in the cleat and matrix systems of coal. *Energy Fuels* **2010**, *24*, 6653–6661.
- (24) Zhao, B.; Wen, G.; Sun, H.; Zhao, X. Experimental Study of the Pore Structure and Permeability of Coal by Acidizing. *Energies* **2018**, *11*, 1162.
- (25) Luo, M. Study on composite permeability increment technology by acid fracturing in low permeability coal seam [Dissertation]. Liaoning Technical University, 2017; pp 65–70.
- (26) Gomaa, I.; Mahmoud, M.; Kamal, M. S. Sandstone Acidizing using a low-reaction acid system. *J. Energy Resour. Technol.* **2020**, *142*, No. 103008.
- (27) Mahmoud, M.; Aljawad, M. S.; Kamal, M. S.; Hussain, S. M. S. Sandstone acidizing using a new retarded acid system based on gemini surfactants. *J. Pet. Sci. Eng.* **2020**, *194*, No. 107459.
- (28) Zhu, D.; Hou, J.; Wang, J.; Wu, X.; Wang, P.; Bai, B. Acid-alternating-base (AAB) technology for blockage removal and enhanced oil recovery in sandstone reservoirs. *Fuel* **2018**, *215*, 619–630.
- (29) Buijse, M.; de Boer, P.; Breukel, B.; Burgos, G. Organic acids in carbonate acidizing. *SPE Prod. Facil.* **2004**, *19*, 128–134.
- (30) Alkhalidi, M. H.; Nasr-El-Din, H. A.; Sarma, H. K. Kinetics of the reaction of citric acid with calcite. *SPE J.* **2010**, *15*, 704–713.
- (31) Mustafa, A.; Aly, M.; Aljawad, M. S.; Dvorkin, J.; Solling, T. A green and efficient acid system for carbonate reservoir stimulation. *J. Pet. Sci. Eng.* **2021**, *205*, No. 108974.
- (32) Jafarpour, H.; Aghaei, H.; Litvin, V.; Ashena, R. Experimental optimization of a recently developed matrix acid stimulation technology in heterogeneous carbonate reservoirs. *J. Pet. Sci. Eng.* **2021**, *196*, No. 108100.
- (33) Schwalbert, M. P.; Aljawad, M. S.; Hill, A. D.; Zhu, D. Decision criterion for acid-stimulation method in carbonate reservoirs: matrix acidizing or acid fracturing? *SPE J.* **2020**, *25*, 2296–2318.
- (34) Luo, M.; Cui, S.; Zhou, X.; Li, S.; Fan, C. Experimental study on permeability enhancement of coal seam with high mineral content by acid fracturing. *Energy Sources, Part A* **2020**, 1–14.

- (35) Chen, S.; Xie, K.; Shi, Y.; Li, Z.; Yang, X.; Cai, J. Chelating agent-introduced unconventional compound acid for enhancing coal permeability. *J. Pet. Sci. Eng.* **2021**, *199*, No. 108270.
- (36) Liu, Z.; Liu, D.; Cai, Y.; Qiu, Y. Permeability, mineral and pore characteristics of coals response to acid treatment by NMR and QEMSCAN: Insights into acid sensitivity mechanism. *J. Pet. Sci. Eng.* **2021**, *198*, No. 108205.
- (37) Tao, S. Dynamic Variation Effects of Coal Reservoir Permeability and the Response of Gas Productivity in Southern Qinshui Basin [Dissertation]. In *China University of Geosciences*; China University of Geosciences (Beijing): Beijing, 2011; pp 35–44.
- (38) Du, Y.; Fu, C.; Pan, Z.; Sang, S.; Wang, W.; Liu, S.; Zhao, Y.; Zhang, J. Geochemistry effects of supercritical CO<sub>2</sub> and H<sub>2</sub>O on the mesopore and macropore structures of high-rank coal from the Qinshui Basin, China. *Int. J. Coal Geol.* **2020**, *223*, No. 103467.
- (39) Li, B.; Zhuang, X.; Querol, X.; Moreno, N.; Córdoba, P.; Li, J.; Zhou, J.; Ma, X.; Liu, S.; Shangguan, Y. The mode of occurrence and origin of minerals in the Early Permian high-rank coals of the Jimunai depression, Xinjiang Uygur Autonomous Region, NW China. *Int. J. Coal Geol.* **2019**, *205*, 58–74.
- (40) Gamson, P. D.; Beamish, B. B.; Johnson, D. P. Coal microstructure and secondary mineralization: their effect on methane recovery. *Spec. Publ. - Geol. Soc. London* **1996**, *109*, 165–179.
- (41) Chen, D.; Pan, Z. J.; Liu, J. S.; Connell, L. D. An improved relative permeability model for coal reservoirs. *Int. J. Coal Geol.* **2013**, *109–110*, 45–57.
- (42) Ham, Y.; Kantzas, A. Measurement of relative permeability of coal: approaches and limitations. In *CIPC/SPE Gas Technology Symposium*; Society of Petroleum Engineers: Calgary, 2008; pp 1–11.
- (43) Zhang, Z.; Yan, D.; Yang, S.; Zhuang, X.; Li, G.; Wang, G.; Wang, X. Experimental studies on the movable-water saturations of different-scale pores and relative permeability of low-medium rank coals from the Southern Junggar Basin. *J. Nat. Gas Sci. Eng.* **2020**, *83*, No. 103585.
- (44) Shen, J.; Qin, Y.; Wang, G. X.; Fu, X.; Wei, C.; Lei, B. Relative permeabilities of gas and water for different rank coals. *Int. J. Coal Geol.* **2011**, *86*, 266–275.